Eur. Phys. J. A **6**, 99–105 (1999)

THE EUROPEAN PHYSICAL JOURNAL A

Formation of η/ω-mesic nuclei using the recoilless (d,^{3}He) reaction

R.S. Hayano[1], S. Hirenzaki[2], A. Gillitzer[3]

[1] Department of Physics, University of Tokyo, Hongo, Bunkyo-ku, Tokyo 113-0033, Japan
[2] Department of Physics, Nara Women's University, Nara 630-8506, Japan
[3] Physik Department E12, Technische Universität München, D-85748 Garching, Germany

Received: 15 February 1999 / Revised version: 21 May 1999
Communicated by Th. Walcher

Abstract. We discuss the possibility to use the recoilless (d,^{3}He) reaction to produce bound states of η and ω mesons in light nuclei. We calculate meson bound states in the nucleus using an optical potential and their formation cross sections with the Green function method, and show that it should be feasible to experimentally observe mesic nuclei in the excitation energy spectrum and to deduce the meson mass shift in nuclei. This method discussed here is complementary to the dilepton invariant-mass spectroscopy, commonly used to study in-medium vector meson masses.

PACS. 25.10.+s Nuclear reactions involving few-nucleon systems – 14.40.Aq π, K, and η mesons – 36.10.Gv Mesonic atoms and molecules, hyperonic atoms and molecules

1 Introduction

The study of in-medium properties of hadrons, modification of meson masses in particular, is one of the most interesting topics of contemporary nuclear physics. Since the in-medium meson masses depend on nuclear density and temperature, and since larger mass-shift effects are expected under extreme conditions, this subject has been often discussed in the context of high energy heavy ion collisions. For example, the results of e^+e^- (CERES) and $\mu^+\mu^-$ (HELIOS-3, NA38) invariant-mass measurements have attracted much attention [1].

Theoretically, Hatsuda and Lee [2] estimated that the ρ and ω masses are about 15% lighter than the vacuum values already at the normal nuclear density ρ_0. A similar mass reduction was obtained by a simple scaling prediction by Brown and Rho [3]. In a recent work by Klingl *et al.* [4,5], they predict that the ω mass gets significantly lighter as the nuclear density is increased, while the ρ meson mass stays almost constant (the ρ meson width, however, is expected to become wider). Since the ω mass is expected to become about $10 \sim 20\%$ lighter at ρ_0 as compared with the vacuum value [2–5], it should be possible to detect this mass shift without using heavy-ion reactions.

The experiments E325 [6] at KEK on p-induced ϕ production and the experiment on π-induced ω production with the HADES spectrometer [7] at GSI are of this category, and they both plan to detect the mass shift by reconstructing e^+e^- decays.

We discuss in this paper an alternative method for studying the in-medium properties of mesons, which is to produce meson-nucleus bound states [8,5] using the recoil-free (d,^{3}He) reaction, and to observe the bound-state peaks in the excitation-energy spectra [9]. So far, no such meson-nucleus bound states have been discovered.

This study is motivated by our recent discovery of deeply-bound pionic states by using the ^{208}Pb(d,^{3}He) reaction [10]. The experiment was done at a beam energy of 600 MeV, close to the recoilless condition, which made it possible to clearly observe the pionic $2p$ state coupled to the ^{207}Pb core with $(p_{3/2})_n^{-1}$ and $(p_{1/2})_n^{-1}$ configurations. By comparing the observed spectrum with theory [11], the pion-nucleus optical potential parameters were determined, from which the effective pion mass of about 160 MeV/c^2 was deduced [12–14] from the relation,

$$[m^{eff}(\rho)]^2 = [m_0^2 + \boldsymbol{q}^2 + Re\Pi(E, \boldsymbol{q}; \rho)]_{q\to 0} \sim m_0^2 + 2m_0 ReU_{opt}^s \ ,$$

where m_0 is the meson mass, Π is the meson self energy and U_{opt}^s is the $s-$wave part of the meson-nucleus optical potential.

Similarly, if meson-nucleus bound state(s) are observed, we can deduce the meson-nucleus potential depth and hence the effective mass; for vector mesons (ρ and ω) as well as heavier pseudo-scaler mesons such as η, the vector part of the potential is expected to be small as compared with the scalar part [15], so that the binding energies can be readily related to the effective mass.

We note that the (d,^{3}He) reaction can realize recoil-free conditions (and hence production of low-angular momentum states) for light mesons, both pseudoscalar (η)

and vector (ρ, ω), but we also note that other conditions have to be met in order for this method to work successfully. Namely,

i) the meson-nucleus attraction must be strong enough to ensure the existence of at least one bound state (unlike the π^- case, there is no assistance of the Coulomb attraction),
ii) the imaginary part of the potential must be moderate, and
iii) the signal cross section must be large enough relative to background continuum.

We show in the following that these conditions can be satisfied both for η and ω-mesic nuclei.

For completeness we note that the (p,d) reaction may also satisfy the recoil free condition at appropriate incident energy, however it does not allow to separate the ejectiles from the beam particles in a magnetic spectrometer due to the same magnetic rigidity in the case of vanishing momentum transfer.

Let us first examine in detail the case of η-mesic nuclei, for which the recoilless condition can be satisfied at GSI-SIS, and then discuss the case of ω-mesic nuclei.

2 η-mesic Nuclei

Existence of η-mesic nuclei was suggested theoretically by Haider and Liu [16]. They systematically investigated η-mesic nuclear states and proposed to use the (π^+, p) reaction for their formation. An experimental attempt to find a bound state in this reaction led to a negative result [17]. The calculation of [16] used a less attractive interaction than the parameters of our choice, and predicted shallower binding and smaller widths than those discussed in the following. The (π^+, p) experiment [17] was designed to be sensitive to the expected narrow state, but was probably not sensitive enough to see a much broader structure.

On the other hand, the cross section for η meson production in d(p,^{3}He)η reactions at threshold was found to be large [18] and was analyzed in terms of a quasi-bound $\eta-^3$He system [19]. For the $\eta-^4$He system also the existence of a quasi-bound state was suggested [20]. Recent theoretical work indicated the existence of η-mesic nuclei, however their structure is only predicted with large uncertainty [21,22]. The existence of η-mesic nuclei is hence still controversial.

In order to study the structure and formation of $\eta-$mesic nuclei, we constructed the η-nucleus optical potential by using the available estimates on the ηN scattering lengths, and used the Green function method to calculate the reaction cross section.

2.1 η-nucleus binding energies

We used the first-order in density η-nucleus optical potential,

$$V_\eta = -\frac{4\pi}{2\mu}\left(1+\frac{m_\eta}{M_N}\right)a_{\eta N}\rho(r), \qquad (1)$$

where $a_{\eta N}$ is the $\eta-$nucleon scattering length, μ is the reduced mass of the η and is $\sim m_\eta$ for heavy nuclei, M_N is the nucleon mass, and ρ is the nuclear density.

There exist several recent estimates on the ηN scattering length:

$$a_{\eta N} = [(0.717 \pm 0.030) + i(0.263 \pm 0.025)]\text{fm [23]}, \quad (2)$$
$$= [(0.751 \pm 0.043) + i(0.274 \pm 0.028)]\text{fm [24]}, \quad (3)$$
$$\approx (0.52 + i0.25)\text{fm [20]}, \quad (4)$$
$$\approx (0.20 + i0.26)\text{fm [25]}. \quad (5)$$

As shown, the first two theoretical estimates agree fairly well with each other. The third value was deduced from an experimental study of d(p,^{3}He)η and d(d,^{4}He)η reactions [20]. In all cases, the η-nucleus optical potential is expected to be attractive. For an illustrative purpose, let us take $\mu = m_\eta = 547$ MeV, $M_N = 939$MeV and $\rho_0 = 0.17\text{fm}^{-3}$ and $a_{\eta N} = 0.717 + 0.263\ i$fm. We then obtain

$$V(r) = -(86 + 32i)\rho(r)/\rho_0 \text{ MeV},$$

which is indeed strongly attractive. The imaginary part $W = -\Gamma/2$ is appreciable, but small enough compared with the real part.

With this potential, we calculated the η-nucleus binding energies and widths for various nuclei in a conventional way of solving the Klein-Gordon equation. The vector part of the potential, which in general must be taken into account, was omitted in these and the following calculations, based on the assumption that the $\eta - N$ interaction is dominated by the $s-$wave component due to the strong coupling to the $N^*(1535)$ resonance. A Woods-Saxon form of the nuclear density profile was used, where nuclear radii and diffuseness were taken to be $R = 1.18A^{1/3} - 0.48$ fm and $a = 0.5$ fm, respectively. The results are shown in Table 1 for the case of $a_{\eta N} = (0.717 + 0.263i)$ fm and in Table 2 for the case of $a_{\eta N} = (0.20 + 0.26i)$ fm. We find that in the former case the half widths are comparable or smaller than the binding energies and/or level spacings, so that it is justified to interpret these states as quasi-stable $\eta-$mesic nuclear bound states.

2.2 Kinematics and cross section

Similar to the case of deeply-bound pionic atom production, it is possible to produce $\eta-$mesic nuclei near the recoilless condition using the (d,^{3}He) reaction on nuclear targets. This is illustrated in Fig. 1, which shows the momentum transfer q vs. the incident deuteron kinetic energy T_d for a typical light target nucleus (^{7}Li in this case). The use of recoilless kinematics is essential to suppress the quasi-free continuum η production and to enhance the $\eta-$mesic nuclear production signal. The recoil-free η condition is satisfied at $T_d \sim 3.6$ GeV.

We now estimate the reaction cross section by using the nuclear response function $S(E)$:

$$\left(\frac{d^2\sigma}{d\Omega dE}\right)_{A(d,^3He)_\eta(A-1)} = \left(\frac{d\sigma}{d\Omega}\right)^{lab}_{p(d,^3He)\eta} \times \sum_{l_\eta, j_n, J} S(E) \qquad (6)$$

Table 1. A-dependence of the η-nucleus binding energies and widths. We use $a_{\eta N} = 0.717 + 0.263i$ $[fm]$ as η-N scattering length.

A	$\ell = 0$		$\ell = 1$		$\ell = 2$		$\ell = 3$	
	B.E.(MeV)	Γ (MeV)	B.E.(MeV)	Γ (MeV)	B.E.(MeV)	Γ (MeV)	B.E.(MeV)	Γ (MeV)
6	17.4	33.5						
11	35.3	48.8						
15	44.4	55.5	9.61	35.9				
19	50.8	59.9	17.7	43.0				
31	62.0	66.3	34.1	55.2	5.87	40.2		
	4.36	34.4						
39	66.4	68.2	40.8	59.1	15.0	48.0		
	11.8	44.5						
64	74.3	71.8	53.3	63.4	31.4	58.8	10.6	52.0
	25.8	58.2						
88	77.6	73.2	61.0	66.8	40.1	59.4	21.4	60.1
	33.3	56.7						
132	80.5	73.2	67.9	70.4	52.6	64.2	32.5	56.9
	47.4	61.4	20.9	53.1				
207	83.0	73.5	72.4	70.1	62.1	69.8	49.5	64.8
	58.5	70.6	43.4	62.1	15.7	39.6		
	11.4	30.4						

Table 2. A-dependence of the η-nucleus binding energies and widths. We use $a_{\eta N} = 0.20 + 0.26i$ $[fm]$ as η-N scattering length.

A	$\ell = 0$		$\ell = 1$		$\ell = 2$		$\ell = 3$	
	B.E.(MeV)	Γ (MeV)	B.E.(MeV)	Γ (MeV)	B.E.(MeV)	Γ (MeV)	B.E.(MeV)	Γ (MeV)
31								
39	5.25	51.9						
64	9.41	57.2						
88	11.7	59.0						
132	14.2	60.6						
207	16.2	61.8	9.09	57.2				

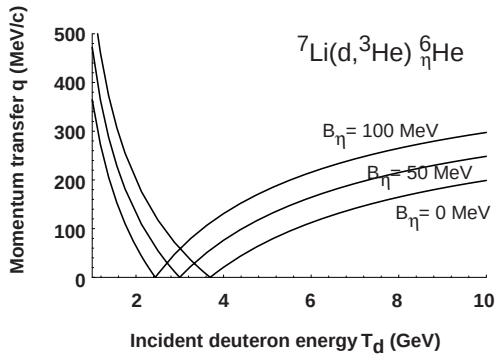

Fig. 1. The momentum transfer q vs. incident deuteron kinetic energy T_d in the ^{7}Li(d,^{3}He)$^6_\eta He$ reaction. The three curves respectively correspond to η binding energies of 100, 50 and 0 MeV, as indicated

where $\left(\frac{d\sigma}{d\Omega}\right)^{lab}_{p(d,^3He)\eta}$ is the elementary cross section in the laboratory frame. A comprehensive and consistent approach to calculate the response function $S(E)$ for a system with a large imaginary potential was formulated by Morimatsu and Yazaki [26]. This method uses the Green function $G(E;\boldsymbol{r},\boldsymbol{r}')$ defined as

$$G(E;\boldsymbol{r},\boldsymbol{r}') =< p^{-1}|\phi_\eta(\boldsymbol{r})\frac{1}{E-H_\eta+i\epsilon}\phi^\dagger_\eta(\boldsymbol{r}')|p^{-1}>, \quad (7)$$

where $\phi^\dagger_\eta$ is the η creation operator and $|p^{-1}>$ is a proton hole state. The Hamiltonian H_η contains the $\eta-$nucleus optical potential. Since we used energy-independent local potentials in the present calculation, we can obtain a simple expression for the Green function as

$$G(E;\boldsymbol{r},\boldsymbol{r}') = \sum_{l_\eta,m_\eta} Y^*_{l_\eta,m_\eta}(\hat{r})Y_{l_\eta,m_\eta}(\hat{r}')G_{l_\eta}(E;r,r') \quad (8)$$

$$G_{l_\eta}(E;r,r') = -2\mu k u_{l_\eta}(k,r_<)v^{(+)}_{l_\eta}(k,r_>), \quad (9)$$

where u_{l_η} and $v^{(+)}_{l_\eta}$ respectively are the radial part of the regular and outgoing solutions of equation of motion. Using the Green function, the response can be calculated as

$$S(E) = -\frac{1}{\pi}Im\sum_{M,m_s} \int d^3r d\sigma d^3r' d\sigma' f^\dagger(\boldsymbol{r},\sigma)G(E;r,r')f(\boldsymbol{r'},\sigma'). \quad (10)$$

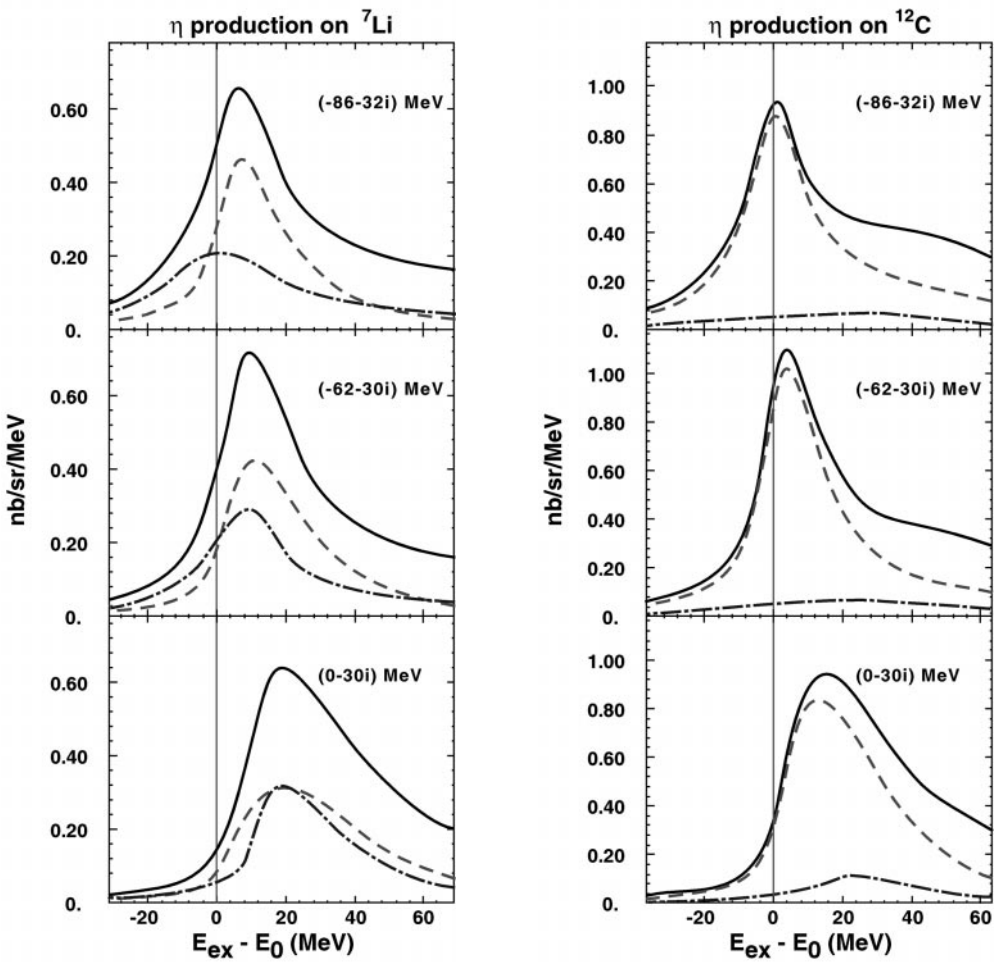

Fig. 2. The calculated excitation energy spectrum of η production in the ^{7}Li(d,^{3}He) reaction (left) and in the ^{12}C(d,^{3}He) reaction (right) at $T_d = 3.5$ GeV, for three different η-nucleus optical potential parameters; (top) $V = -(86 + 32i)\rho/\rho_0$ MeV, (middle) $V = -(62 + 30i)\rho/\rho_0$ MeV, (bottom) $V = -30i\rho/\rho_0$ MeV. The vertical lines indicate the η production threshold energies. In each figure, the contribution from the $(0p_{3/2})_p^{-1} \otimes p_\eta$ is shown in a dashed curve, the $(0s_{1/2})_p^{-1} \otimes s_\eta$ contribution is shown in a dash-dotted curve, and the solid curve is the sum of η-partial waves up to $l = 6$. The continuum background contributions are estimated to be about 2.7 nb/sr/MeV for the ^{7}Li target and 3.4 nb/sr/MeV for the ^{12}C target (see text).

We define $f(\boldsymbol{r}, \sigma)$ as

$$f(\boldsymbol{r}, \sigma) = \chi_f^*(\boldsymbol{r}) \xi^*_{\frac{1}{2}, m_s}(\sigma) [Y^*_{l_\eta}(\hat{r}) \otimes \psi_{j_p}(\boldsymbol{r}, \sigma)]_{JM} \chi_i(\boldsymbol{r}), \quad (11)$$

where χ_i and χ_f respectively denote the projectile and the ejectile distorted waves, ψ is the proton hole wavefunction and ξ is the spin wavefunction introduced to count possible spin directions of the proton in the target nucleus. The numerical values of $S(E)$ were evaluated by using the eikonal approximation as in the case of deeply-bound pionic atoms [27].

The elementary cross section for η production which appears in (6) can be inferred from the energy dependence of the p(d,^{3}He)η cross section measured at SATURNE [28] in the d(p,^{3}He) reaction. At $T_p = 1.75$ GeV (this proton kinetic energy corresponds to the recoilless η production in the p(d,^{3}He)η reaction), the c.m. cross section $(d\sigma/d\Omega)_{cm}$ is 3 nb/sr. This can be translated to the $d+p$ laboratory-frame cross section via

$$\frac{d\sigma}{d\Omega}_{lab} = \left(\frac{p_{lab}(^3\mathrm{He})}{p_{cm}(^3\mathrm{He})} \right)^2 \frac{d\sigma}{d\Omega}_{cm}, \quad (12)$$

and the approximate elementary cross section was deduced to be 150 nb/sr.

2.3 (d,^{3}He) spectra

In Fig. 2, we show the calculated excitation-energy (E_{ex}) spectra using the Green function method described above. The results are shown for the ^{7}Li target (left panel) and for the ^{12}C target (right panel), for different potential parameters. The top and middle figures respectively correspond to the ηN scattering lengths of (2) ($V(r) = -(86 + 32i)\rho(r)/\rho_0$ MeV) and (4) ($V(r) = -(62 + 30i)\rho(r)/\rho_0$ MeV). The bottom figures are for the potential with no binding, $V(r) = -30i\rho(r)/\rho_0$ MeV.

In solid lines, the expected double-differential forward (0°) cross sections are shown. The dashed and dash-dotted lines respectively show the contributions from the $(p_{3/2})_p^{-1} \otimes (2p)_\eta$ and the $(s_{1/2})_p^{-1} \otimes (1s)_\eta$ substitutional configurations. These two configurations contribute dominantly to the energy spectra, although we in fact calculated contributions from other partial waves (up to $l = 6$) and confirmed that there are no significant contributions from partial waves beyond $l = 6$.

The vertical lines indicate the η production threshold energies (E_0). The η binding energy B_η for these light $p-$shell nuclei can be deduced from the excitation energy as (for the sake of simplicity we ignore the nuclear recoil energy, which is small near the recoilless condition):

$$E_{ex} = m_\eta c^2 - B_\eta + (S_p(j_p) - S_p(p_{3/2})), \qquad (13)$$

where $(S_p(j_p) - S_p(p_{3/2}))$ is the proton hole energy measured from the ground state of the residual nuclei. Hence, for the η states coupled to the $(s_{1/2})_p^{-1}$ configuration, the $(s_{1/2})_p^{-1} - (p_{3/2})_p^{-1}$ energy differences (14 MeV for ^{7}Li and 18 MeV for ^{12}C) taken from [29] was added when calculating these spectra.

Note that the ground state of the $\eta-$nucleus system for these light $p-$shell targets would have the $(p_{3/2})_p^{-1} \otimes (1s)_\eta$ configuration, but this component does not contribute to the energy spectra near the recoilless condition. Instead, the dominant contribution comes from the $(p_{3/2})_p^{-1} \otimes (2p)_\eta$ configuration, and we can determine the $\eta-$nucleus potential from the location of the $2p$ peak. This $(p_{3/2})_p^{-1} \otimes (2p)_\eta$ component is more dominant in the ^{12}C case because there are four $p_{3/2}$ protons in a ^{12}C nucleus as compared to only one in a ^{7}Li nucleus.

In Fig. 3, we show the calculated spectrum for a heavier target, ^{40}Ca. The potential strength corresponds to the scattering length in (4). Due to the recoilless condition, dominant contributions come from the substitutional states. However, as can be seen in the figure, several proton-hole states contribute to a broad maximum in the excitation-energy spectrum which makes the interpretation difficult. We therefore conclude that light nuclei like those in the p-shell region are most suitable to search for bound nuclear states of η mesons.

2.4 Background considerations

The continuum background for η production in the elementary process was estimated by using the $pd \to \eta^3$He data by Berthet et al. [28] to be

$$d^2\sigma/dEd\Omega_{lab} \sim 4.5\text{nb/sr/MeV}$$

at $T_d = 4$ GeV.

We then calculated the distortion effects of the deuteron and the ^{3}He in the target nucleus, in order to estimate the continuum background level in the case of nuclear targets. This was done by summing up the effective numbers for all final state configurations of proton-hole and mesonic states. The calculated effective proton numbers had negligible energy dependence. We further assumed that the contributions of target protons and neutrons to the background are identical, and hence we multiplied the calculated effective numbers by a factor A/Z. These total effective numbers, 0.59 for ^{7}Li and 0.75 for ^{12}C, are expected to be good estimations of the distortion effects to the projectile and the ejectile. And this is also expected to be consistent with the estimation of signal cross sections. The constant background levels thus estimated are 2.7 nb/sr/MeV for ^{7}Li and 3.4 nb/sr/MeV for ^{12}C. It should be feasible to clearly observe the η production signal with the peak cross section of $0.6 \sim 1.0$ nb/sr/MeV (Fig. 2) on top of such a continuum background.

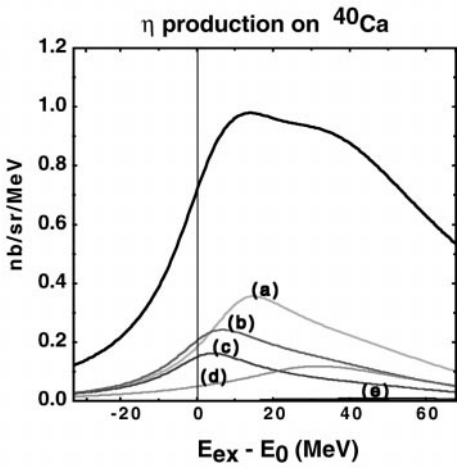

Fig. 3. The calculated excitation energy spectrum of η production in the ^{40}Ca(d,^{3}He) reaction at $T_d = 3.5$ GeV, for $V = -(62 + 30i)\rho/\rho_0$ MeV. The labelled curves denote contributions from the following configurations: a) $[(1d_{5/2})_p^{-1} \otimes d_\eta]$, b) $[(1d_{3/2})_p^{-1} \otimes d_\eta]$, c) $[(2s)_p^{-1} \otimes s_\eta]$, d) $[(1p)_p^{-1} \otimes p_\eta]$ and e) $[(1s)_p^{-1} \otimes s_\eta]$.

2.5 Experimental feasibility

In Fig. 4, we show expected excitation-energy spectra for the ^{7}Li case assuming 100 hours of beam time at GSI, using the FRS as ^{3}He spectrometer. As shown, we expect the peaks to be clearly visible above background, and the spectra are sensitive enough to differentiate between various $\eta-$nucleus potential parameters. The experimental setup will be similar to the one used for the study of deeply-bound pionic atoms. For the estimate we used a target thickness of 1g/cm^2, a deuteron beam intensity of 3×10^{10}/sec at 3.5 GeV incident energy, and $\Omega = 2.5 \times 10^{-3}$sr for the FRS acceptance; all these parameters are achievable at GSI.

3 ω-mesic nuclei

Here, we would like to mention that the (d,^{3}He) reaction is also well-suited for the production of ω-mesic nuclei. In

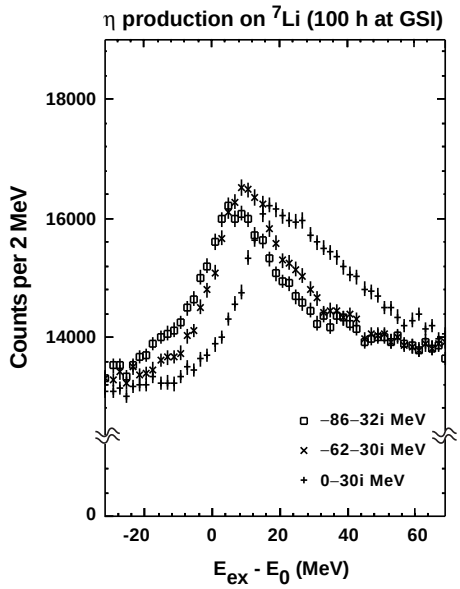

Fig. 4. Expected excitation energy spectrum for the ^{7}Li(d,^{3}He) reaction near the η production threshold for 100 hours of running at GSI (see text for assumptions of the experimental conditions).

Fig. 5, we show calculated excitation-energy spectra for ω production in the (d,^{3}He) reaction on ^{7}Li at $T_d = 3.8$ GeV (also possible at GSI).

In the top panel of Fig. 5, the real part of the potential was set to be $V(r) = -100\rho(r)/\rho_0$ MeV based on the 15% mass reduction of ω at normal nuclear density. We chose the imaginary part to be $W(r) = -70\rho(r)/\rho_0$ MeV based on the ω lifetime ($\tau = 1.5$fm$/c$) in nuclear medium at $\rho = \rho_0$ [4], *i.e.*, $W = -\Gamma/2 = 1/2\tau \sim -70$ MeV. The dependence of the spectral shape on the potential parameters are indicated in the middle and bottom panels of Fig. 5.

The elementary cross section was estimated to be 450 nb/sr, by translating the d(p,^{3}He)ω data taken at SATURNE [30] to the $d+p$ laboratory-frame cross section with (12). The rest of the calculations were carried as in the η case. The d(p,^{3}He)ω data [30] was also used to calculate the continuum background level, which we estimated to be 7.7 nb/sr/MeV.

At this incident energy, however, the recoilless condition is not satisfied, and we hence find that the contributions from substitutional states are not dominant, and that the quasi-free process makes a large contribution in the unbound region. Although the identification of bound states appears to be difficult, the effect of an attractive ω-nucleus potential is noticeable in the bound region of the excitation-energy spectrum.

In order to see the effect of the recoil free condition for ω production we show in Fig. 6 the calculated spectrum at 10 GeV incident deuteron energy. Since there is no experimental data available which can be used to estimate the elementary cross section at this energy, we assumed the elementary ω production cross section to be

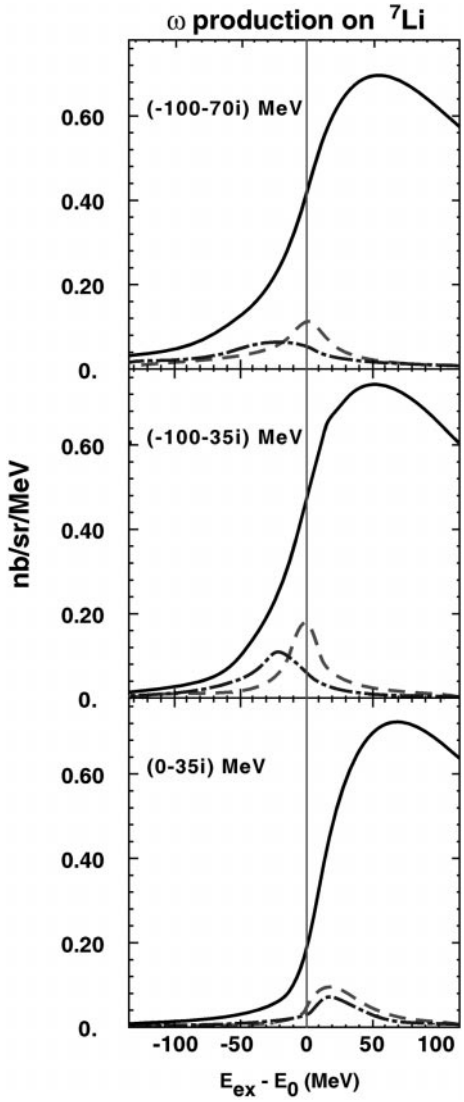

Fig. 5. The calculated excitation energy spectra of ω production in the ^{7}Li(d,^{3}He) reaction at $T_d = 3.8$ GeV, for three different ω-nucleus optical potential parameters; (top) $V = -(100 + 70i)\rho/\rho_0$ MeV, (middle) $V = -(100 + 35i)\rho/\rho_0$ MeV, (bottom) $V = -35i\rho/\rho_0$ MeV. The vertical lines indicate the ω production threshold. In each figure, the contribution from the $(0p_{3/2})_p^{-1} \otimes p_\omega$ is shown in a dashed curve, the $(0s_{1/2})_p^{-1} \otimes s_\omega$ contribution is shown in a dash-dotted curve, and the solid curve is the sum of partial waves up to $l = 6$. The continuum background contributions are estimated to be about 7.7 nb/sr/MeV.

450 nb/sr. In this case, as in the η-production spectrum at $T_d = 3.5$ GeV, the dominant contributions result from substitutional states. With less configurations contributing the ω-nucleus optical potential may be deduced from the spectral shape more directly.

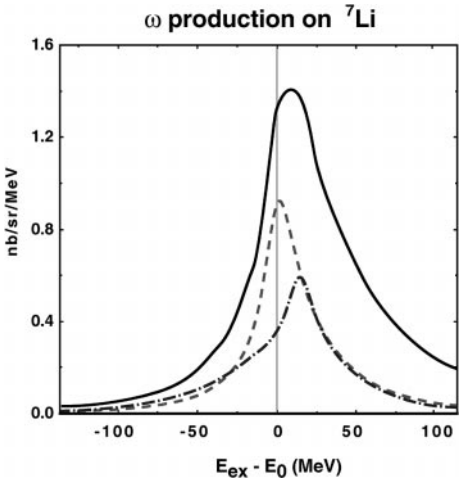

Fig. 6. The calculated excitation energy spectrum of ω production in the ^{7}Li(d,^{3}He) reaction at $T_d = 10$ GeV. The potential was assumed to be $V(r) = -(100 + 70i)\rho(r)/\rho_0$ MeV. The elementary cross section was assumed to be 450 nb/sr. The contribution from the $(0p_{3/2})_p^{-1} \otimes p_\eta$ is shown in a dashed curve and the $(0s_{1/2})_p^{-1} \otimes s_\eta$ contribution is shown in a dash-dotted curve. The solid curve is the sum of $\omega-$partial waves up to $l = 6$.

4 Conclusions

In conclusion, we find that the recoilless (d,^{3}He) reaction is a promising tool to study the $\eta-$nucleus system, and we should be able to determine the $\eta-$nucleus potential (and the possible η mass shift in nuclei) from the excitation-energy spectra. This method can be extended to study the behavior of other mesons such as ω in nuclei.

The method discussed here is complementary to studies of vector mesons in nuclear matter by analyzing their invariant mass spectrum in the dilepton decay channel, such as $\omega \to e^+e^-$.

The authors would like to thank H. Toki, T.-S. H. Lee, K. Itahashi, H. Gilg, F. Klingl, T. Waas, W. Weise, P. Kienle and T. Yamazaki for helpful discussions. This work is supported in part by the Grant-in-Aid for Scientific Research, Monbusho, Japan.

References

1. Recent results are summarized in, for example, I. Tserruya, Nucl. Phys. A638 365c (1998).
2. T. Hatsuda and S. H. Lee, Phys. Rev. C46 R34 (1992).
3. G.E. Brown and M. Rho, Phys. Rev. Lett. 66, 2720 (1991).
4. F. Klingl, N. Kaiser, W. Weise, Nucl. Phys. A624 527 (1997)
5. F. Klingl, T. Waas and W. Weise, nucl-th/9810312, Nucl. Phys. A (in print). This paper gives an updated $\omega - N$ scattering length over the value given in [4].
6. S. Yokkaichi et al., Nucl. Phys. A638 435c (1998).
7. The HADES collaboration, Proposal for a High Acceptance Di-Electron Spectrometer, GSI 1994.
8. K. Saito, K. Tsushima, D.H. Lu, A.W. Thomas, nucl-th/9807028, Phys. Lett. B (in print).
9. An experimental proposal based on this study has been approved at GSI: R. S. Hayano, A. Gillitzer et al., GSI proposal S214 (1997).
10. T. Yamazaki et al., Z. Phys. A355 219 (1996).
11. S. Hirenzaki, H. Toki, T. Yamazaki, Phys. Rev. C44 2472 (1991).
12. T. Waas, R. Brockmann, and W. Weise, Phys. Lett. B405 215 (1997).
13. T. Yamazaki et al., Phys. Lett B418 246 (1998).
14. E. Friedman and A. Gal, Phys. Lett. B 432, 235 (1998).
15. K. Saito, K. Tsushima, A.W. Thomas, Phys. Rev. C55 2637 (1997); *ibid.* C56 566 (1997).
16. Q. Haider and L. C. Liu; Phys. Lett. B172(1986)257, Phys. Rev. C34 1845 (1986).
17. R. E. Chrien et al., Phys. Rev. Lett 60 2595 (1988).
18. J. Berger et al., Phys. Rev. Lett. 61 919 (1988).
19. C. Wilkin, Phys. Rev. C47 R938 (1993).
20. N. Willis et al., Phys. Lett B406 14 (1997).
21. H. C. Chiang, E. Oset, and L. C. Liu, Phys. Rev. C44 738 (1991).
22. S. A. Rakityansky et al., Phys. Rev. C53 R2043 (1996).
23. M. Batinić *et al.* nucl-th/9703023. This is an update to their original work published in Phys. Rev. C51 2310 (1995) and its erratum, Phys. Rev. C57 1004 (1998).
24. A.M. Green, S. Wycech, Phys. Rev. C55 R2167 (1997).
25. N. Kaiser, T. Waas, W. Weise, Nucl. Phys. A612 297 (1996).
26. O. Morimatsu and K. Yazaki, Nucl. Phys. A435 (1985) 727; Nucl. Phys. A483 493 (1988).
27. H. Toki, S. Hirenzaki and T. Yamazaki, Nucl. Phys. A530 679 (1991).
28. P. Berthet *et al.*, Nucl. Phys. A443 589 (1985).
29. S.L. Belostotskii *et al.*, Sov. J. Nucl. Phys. 41 903 (1985).
30. R. Wurzinger *et al.*, Phys. Rev. C51 R443 (1995).